JCTC Journal of Chemical Theory and Computation

Article

pubs.acs.org/JCTC

Polarizable Site Charge Model at Liquid/Solid Interfaces for Describing Surface Polarity: Application to Structure and Molecular Dynamics of Water/Rutile TiO_2(110) Interface

Hisao Nakamura,*,† Tatsuhiko Ohto,‡,§ and Yuki Nagata*,‡

†Nanosystem Research Institute (NRI), "RICS," National Institute of Advanced Industrial Science and Technology (AIST), Central 2, Umezono 1-1-1, Tsukuba, Ibaraki 305-8568, Japan

‡Max-Planck Institute for Polymer Research, Ackermannweg 10, 55128, Mainz, Germany

§Department of Chemical System Engineering, Graduate School of Engineering, the University of Tokyo, Tokyo 113-8656, Japan

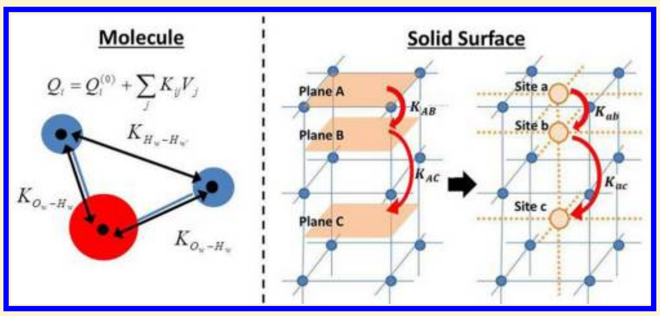

ABSTRACT: We present a novel scheme to construct a polarizable force field for liquid/solid interfaces, which takes into account the effect of the surface polarity induced by liquid−solid interactions explicitly. We extend the charge response kernel (CRK) method for molecules to solid surfaces by introducing the surface CRK. The CRK parameters are systematically determined by the first-principles calculations in the slab model with the dipole-correction method. Our methodology is applied to the water/clean rutile TiO_2(110) interface. Structures and induced charges of a single water molecule attached to the TiO_2 surface optimized by our polarizable force field show good agreement with those predicted by the first-principles calculations. Further, we carried out MD simulations for the liquid water/TiO_2 interface and found three stable structures of water attached to the TiO_2 surface. Two of them are predicted by both the polarizable and the nonpolarizable force fields, while the polarizable force field model predicts a structure of water with the hydrogen and oxygen atoms interacting with the oxygen atom of the surface TiO_2 and the hydrogen atom of the other water molecule, respectively, which was reported by the previous first-principles MD simulation. This indicates that the dipole moments of water and TiO_2 induced by the water−TiO_2 interactions have significant impact on molecular conformations of the water/TiO_2 interface.

I. INTRODUCTION

Liquid/solid interfaces offer unique environments for inhomogeneous catalytic reactions and electrode reactions. Complex liquid−solid interactions often lower the activation energies of reactions, and as a result the reactions are accelerated at the liquid−solid interfaces compared with the bulk liquids. Over past years, water/rutile TiO_2(110) surfaces have become one of the most intriguing liquid/solid interfaces because of the superhydrophilic and photocatalytic properties of the TiO_2 surface.[1,2] Many industrial applications such as self-cleaning coating and photocatalytic oxidization have enhanced the interest in the water/TiO_2 interfaces. Understanding the structure and dynamics of water near the TiO_2 surfaces is, thus, crucial to reveal the underlying mechanisms of these properties at the water/TiO_2 interfaces and to gain further efficiency of the photocatalytic reactions.

First-principles molecular dynamics (MD) simulations are powerful tools to study dynamical properties such as viscosity and diffusion constants in condensed systems. They have been applied to the water/rutile and anatase TiO_2 interfaces to investigate the molecular structures[3−10] and electrochemical properties.[11,12] However, due to its high computational cost, first principles MD simulations for the water/TiO_2 interfaces have been limited up to 100 ps with a surface area of ∼13 Å × 13 Å. MD trajectories up to nanoseconds are required to monitor water dynamics.[10] Since MD simulations with the force-field models are computationally inexpensive, it would provide a practical approach to investigate the water structure and dynamics near the TiO_2 surface.[13,14]

Several force fields have been proposed to reproduce the structures of water attached to the TiO_2 surface obtained from the first-principles calculations.[15,16] The Hamiltonian of the force-field models for liquid/solid interfacial systems can be written as

$$H = K + V_S + V_L + V_{L-S} \tag{1}$$

where K represents the kinetic energy, V_S and V_L represent the potential energies for solid and liquid, respectively, and V_{L-S} represents the liquid−solid interaction energy.[15−17] Since a site charge located at each atom position is fixed in the nonpolarizable force-field models,[15,16] the variations of the dipole moments of liquids near solid surfaces and the surface dipoles in solids induced by liquids have not been taken into consideration. Induced dipole moments at the interfaces affect the structures of adsorbed molecules[18,19] and interfacial water,[20] indicating that MD simulations that incorporate the polarization effects are required

Received: November 14, 2012
Published: December 31, 2012

to simulate liquid/solid interfaces. Polarizable force fields for the bulk TiO_2 have been developed to describe the charge induced by the morphology change.[21−25] However, accuracy of the MD simulations by employing the polarizable force fields of water and bulk TiO_2 is questionable, because the charges in these bulk TiO_2 force fields are designed to respond to an internal electric field associated with the TiO_2 morphology rather than an external electric field generated by water. The complexity for modeling liquid/solid interfaces with a polarizable model also arises from the different treatment of the electrostatic interactions; the nearest-neighbor (1−2) and second nearest-neighbor (1−3) bonded electrostatic interactions are described by the harmonic bond stretch and angle bending interactions, respectively, in the conventional force fields for liquids, V_L (Amber,[26] OPLS,[27] Charmm,[28] and so on), while the electrostatic interactions for all the atom pairs are calculated in the force fields for bulk solids, V_S. Hence, a polarizable force field for describing the liquid−solid interaction potential, V_{L-S}, should be constructed independent of V_S and V_L.

In this paper, we present a MD simulation protocol to describe the surface polarity at liquid/solid interfaces by using the charge response kernel (CRK) approach.[29,30] Though the CRK has been used to describe the polarization effects for molecular systems,[31−34] the direct application of the CRK to solids like semiconductor or metal bulk has fundamental difficulty due to the nonlocality of the electronic charge. We extend the CRK scheme to solid surface systems, where the CRK parameters are obtained from the first-principles calculation of a periodic slab model with the dipole-correction method.[35,36] We apply our CRK scheme to the water/TiO_2 interface and construct a new polarizable force field for describing the water−TiO_2 interactions. To check our force-field model, the optimized geometry of a single water molecule on the TiO_2 surface is compared between our polarizable force field and the first-principles calculation. Furthermore, since the polarizable force field can provide information on the induced charges, we compare the axial distribution of the induced charges of water and the TiO_2 surface between our model and first-principles calculations. Then, we perform the MD simulation of *liquid* water/TiO_2 and discuss the stable *liquid* water structures near the TiO_2 surface.

This article is organized as follows. Section II describes a protocol to construct a polarizable force field for describing liquid−solid interactions. In section III, this protocol is applied to the water/clean rutile TiO_2 interface. In section IV, a single water molecule attached to the TiO_2 surface predicted by our force-field model is compared with the first-principles calculation. The structure of *liquid* water near the TiO_2 surface is analyzed in section V. Concluding remarks are given in section VI.

II. GENERAL THEORY FOR POLARIZABLE FORCE FIELD TECHNIQUE AT LIQUID/SOLID INTERFACES

II.A. CRK Model. The CRK is classified to the dynamic charge model.[37] In the CRK model, a site charge responds linearly to an electrostatic potential acting on a site. The charge is determined by the self-consistent field (SCF) equations[29,30]

$$q_i = q_i^{(0)} + \sum_j K_{ij} V_j \tag{2}$$

$$V_i = \sum_j \frac{q_j}{r_{ij}} f_{\mathrm{Thole}}(r_{ij}) \tag{3}$$

where zeroth order charge $q_i^{(0)}$ is the gas-phase charge at site i, K_{ij} is the CRK connecting sites i and j, and V_i is the electrostatic potential acting on site i. To avoid divergence of induced charges, we introduced Thole's damping function

$$f_{\mathrm{Thole}}(r_{ij}) = \begin{cases} 1 \text{ for } x \geq 1 \\ x^4 - 2x^3 - 2 \text{ for } x < 1 \end{cases} \tag{4}$$

where $x = r_{ij}/A(\alpha_i \alpha_j)^{1/6}$ and α_i was the polarizability volume of the site i.[38] A was set to 2.8.[32] The electrostatic interaction potential can be recast as

$$V_{\mathrm{ele}} = \sum_{i>j} \frac{q_i q_j}{r_{ij}} f_{\mathrm{Thole}}(r_{ij}) + \frac{1}{2} \sum_{i,j} V_i K_{ij} V_j \tag{5}$$

The CRK model has been successfully applied to molecular systems such as water,[32] protein,[31] and ionic liquids.[34] One of the advantages in the CRK model is that the CRK parameters can be determined from the first-principles calculations directly. We have proposed an easy-to-implement methodology to calculate the CRK parameters.[33] In this methodology, $q_i^{(0)}$ is given by the electrostatic potential (ESP) fitted charges q_i^{ESP} without an external electric field, while the CRK parameters can be obtained from the ESP charges under the external electric fields of $+\Delta F$ and $-\Delta F$ by performing the least-squares fitting for

$$\Delta q_i^{\mathrm{ESP}} = \sum_j K_{ij} \Delta V_j \tag{6}$$

where $\Delta q_i^{\mathrm{ESP}} = (q_i^{\mathrm{ESP}}|_{\Delta F} - \Delta q_i^{\mathrm{ESP}}|_{-\Delta F})/2$ and $\Delta V_i = (V_i|_{\Delta F} - V_i|_{-\Delta F})/2$.

However, applying this procedure to solid surfaces is not straightforward for the following two reasons. First, unlike in molecular liquids, charges in solids induced by an external electric field (for example, an electric field generated by liquids) are delocalized and, thus, an ESP charge at each atom site is not suitable for characterizing an induced surface charge in solids. Second, since solid surfaces are essentially semi-infinite with two-dimensional periodicity, surface charges should be calculated with physically reasonable boundary conditions, which are required so that surface charges calculated in a microscopic system are consistent with the macroscopic surface charges defined in terms of the electromagnetism of a condensed medium. In the following, a procedure to model the surface polarity from the first-principles calculations is given.

II.B. Extension of CRK for Solid Surface System. In this paper, the "minimum sample cell" denotes a minimum cell large enough to calculate the macroscopic polarization. The "minimum sample slab" can be created by stacking the minimum sample cells. In the linear response regime, the polarization field is expressed as

$$P(z, \omega) = \chi(z, \omega) E(z, \omega) \tag{7}$$

where P, χ, and E are the polarization, susceptibility, and electric field, respectively. The z axis is the surface normal, and the xy plane is parallel to the surface. E is averaged along the x and y directions. Since polarizable force fields assume the Born−Oppenheimer approximation, we set $\omega \to 0$. When P is obtained as a function of z, the induced charge density $\rho^{\mathrm{ind}}(z)$ is calculated by

$$\rho^{\mathrm{ind}}(z) = -\frac{dP(z)}{dz} \tag{8}$$

The induced charge per boundary surface area (S_0) of the minimum sample cell can be mapped from the induced charge density by using a smooth Gaussian function

$$q^{\mathrm{ind}}(z_0) = S_0 \int dz \exp\left(-\frac{(z - z_0)^2}{2\sigma^2}\right) \rho^{\mathrm{ind}}(z) \tag{9}$$

dx.doi.org/10.1021/ct300998z | J. Chem. Theory Comput. 2013, 9, 1193−1201

where $q^{\mathrm{ind}}(z_0)$ is an induced charge distributed on the $z = z_0$ surface and σ is a Gaussian width. To extend the CRK scheme to a surface system, we introduced the surface CRK (SCRK), which represented charge transfer from surface A to surface B

$$K_{\mathrm{AB}}^{\mathrm{SCRK}} = q_{\mathrm{A}}^{\mathrm{ind}}/V_{\mathrm{B}} \tag{10}$$

The electrostatic potential at surface B, V_B, can be calculated from an asymptotic electric field E in the vacuum region.

Unlike isolated molecules, the surface dipole in solids induced by the applied electrostatic field E^{app} contributes to the whole electric field E. Thus, E should be calculated in a self-consistent way. In the dipole-correction method, the SCF calculations are performed in a uniform external field and the depolarization field in the slab is added to E.[35,36] In the present study, we adopted a similar strategy to that reported in ref 36, where the electrostatic potential term in the Kohn–Sham Hamiltonian was written as the sum of the saw potential V^{saw} and the Hartree potential V^{H}

$$V(\vec{r}) = V^{\mathrm{H}}(\vec{r}) + V^{\mathrm{saw}}(z) \tag{11}$$

V^{saw} is given by

$$V^{\mathrm{saw}}(z) = -e\left(\frac{4\pi m_z}{L_0} - E^{\mathrm{app}}\right)z \tag{12}$$

where m_z is the slab dipole moment along the surface normal and L_0 is the length of the supercell in the z direction. Since m_z is calculated by the charge density, it is updated every iterative SCF step. In this way, the asymptotic electric field includes the response of solids.

Sequentially, the SCRK is mapped onto the CRK, because site charges can be easily dealt with in the MD simulations compared with the surface charges. The CRK sites should be located at the centers of the Gaussian functions in eq 9 and are not necessarily the same as the atom sites. In fact, it is well-known that the center of the Wannier orbital strongly depends on each orbital character of the solids, and the maximum charge density points are often not close to the atom sites in solids due to the delocalized charge density.[39,40] The calculation procedures are summarized in Figure 1.

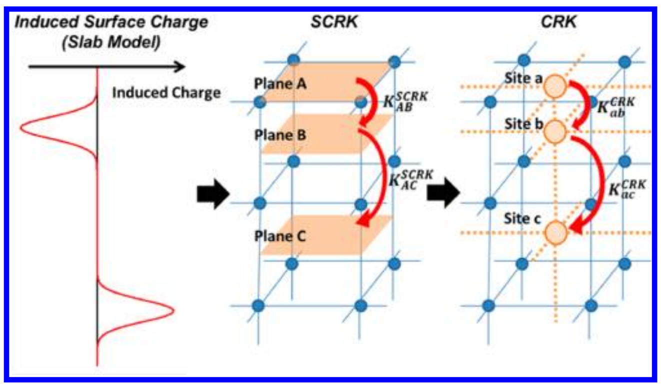

Figure 1. Calculation scheme for the SCRK and CRK for the solid surfaces.

At the end of this section, we describe an analogy of our polarizable site charge model with the modern solid state theory. Stengel has discussed the polarization in bulk solids based on Tasker's model.[41,42] Following ref 41, the polarity at the surface can be calculated by summing up the dipole moments of minimum sample slabs as

$$P = \sum_{i \in \mathrm{atom\ site}} q_i R_i + \sum_{j \in WI} q_j R_j \tag{13}$$

where q is the site charge and R is the position of site i. Sites i and j represent an atom site and a Wannier ion (WI) site, respectively. The second term is required for describing delocalized electric structures in solids.[41] In our polarizable force field model for liquid/solid interfaces, we have decomposed the total solid polarity into the permanent polarity and the polarity induced by an external electric field by liquids

$$P = \sum_{i \in \mathrm{atom\ site}} q_i^{\mathrm{eff}} R_i + \sum_{j \in \mathrm{WI}} q_j^{\mathrm{ind}} R_j \tag{14}$$

where q_i^{eff} is given by the nonpolarizable force field model of ref 16 and q_j^{ind} is calculated within the CRK model. When the Stengel model (eq 13) is compared with our force field model (eq 14), one can see that locating the CRK sites at the nonatom sites of solids in our modeling is consistent with Stengel's approach. Furthermore, this formalism expressed by eq 14 allows us to incorporate the polarizable charge model into well-established nonpolarizable force field models. Hereafter, we call a CRK site in solids a WI site to distinguish it from a CRK site for molecular systems.

III. APPLICATION TO THE WATER/TiO_2 INTERFACE

III.A. Polarizable Force Field for Water/TiO_2 Interface.

We shall apply the CRK model to the water/TiO_2 interface. The atom types for our polarizable force field are listed in Table 1.

Table 1. List of Atom Type for the Water/TiO_2 System

type	description
O_w	oxygen atom of water
H_w	hydrogen atom of water
Ti	Ti atom in the bulk TiO_2
Ti_V	5-fold coordinate titanium atom on the Ti surface layer
Ti_{VI}	6-fold coordinate titanium atom on the Ti surface layer
O	oxygen atom in the bulk TiO_2
O_s	oxygen atom on the Ti surface layer
O_u	3-fold coordinated oxygen atom next to the Ti surface layer
O_b	2-fold coordinated oxygen atom next to the Ti surface layer
W	CRK site in the bulk TiO_2
W_b	CRK site at the position of O_b
W_s	CRK site on the Ti surface layer

The potential energy terms for the water/clean rutile TiO_2(110) interface are given by

$$V_S = V_{\mathrm{TiO_2,BH}} + V_{\mathrm{TiO_2,ele}} \tag{15}$$

$$V_L = V_{\mathrm{water,LJ}} + V_{\mathrm{water,ele}} + V_{\mathrm{water,intra}} \tag{16}$$

$$V_{\mathrm{L-S}} = V_{\mathrm{water-TiO_2,BH}} + V_{\mathrm{Ow-Ob,LJ}} + V_{\mathrm{water-TiO_2,ele}} \tag{17}$$

where the Buckingham and Lennard-Jones potentials are given by

$$V_{\mathrm{BH}} = \sum_{i>j} \left(A_{ij} \exp\left(-\frac{r_{ij}}{\rho_{ij}}\right) - C_{ij}\frac{1}{r_{ij}^6}\right) \tag{18}$$

and

$$V_{\mathrm{LJ}} = \sum_{i>j} 4\epsilon_{ij}\left(\left(\frac{\sigma_{ij}}{r_{ij}}\right)^{12} - \left(\frac{\sigma_{ij}}{r_{ij}}\right)^{6}\right) \tag{19}$$

respectively. The Buckingham potential parameters of $V_{\mathrm{TiO_2,BH}}$ and $V_{\mathrm{water-TiO_2,BH}}$ are given by ref 16. For the O_w–O_b interaction

dx.doi.org/10.1021/ct300998z | J. Chem. Theory Comput. 2013, 9, 1193–1201

potential, we used the Lennard-Jones potential $V_{\text{Ow-Ob,LJ}}$ with σ = 3.166 Å and ε = 0.155 kcal/mol instead of the Buckingham potential. The Lennard-Jones parameters of water are given by ref 43. The polarizable electrostatic potential $V_{\text{water,ele}}$ has the form of eq 5, and $q_i^{(0)}$ and K_{ij} are given in Tables 2 and 3, respectively. $V_{\text{TiO}_2\text{,ele}}$ is given by

Table 2. Charges and Polarizability Volumes in the Atomic Unit

	$q^{(0)}$ (e)	α (au)
O_w	−0.6810[a]	5.8171[c]
H_w	0.3405[a]	3.4686[c]
Ti	2.1960[b]	10.2739[d]
Ti_V	2.1560	10.2739
Ti_{VI}	2.1560	10.2739
O	−1.0980[b]	2.9314[d]
O_b	−1.0180	2.9314
O_s	−1.0980	2.9314
O_u	−1.0980	2.9314
W_b	0.0000	2.9314
W_s	0.0000	2.9314
W	0.0000	2.9314

[a]Ref 43. [b]Ref 16. [c]Ref 38. [d]Ref 22.

Table 3. Off-Diagonal CRK Parameters

CRK pair		K (au)	
O_w	H_w	−2.7090	
H_w	$H_{w'}$	0.4949	
W_b	W_s	−1.1664	
W_s	$W_{s'}$	−0.2287[a]	(−1.8522[b])
W_s	W	−0.9883	
W	W′	−0.4574[c]	(−0.3704[b])

[a]CRK in the x direction. [b]CRK in the y direction. [c]CRK in the x and z directions.

$$V_{\text{TiO}_2\text{,ele}} = \sum_{i>j} \frac{q_i^{\text{eff}} q_j^{\text{eff}}}{r_{ij}} \tag{20}$$

while the polarizable electrostatic potential $V_{\text{water–TiO}_2\text{,ele}}$ is expressed by

$$\begin{aligned} V_{\text{water–TiO}_2\text{,ele}} = & \sum_{i\in \text{water}} \sum_{j \in \text{atom site in TiO}_2} \frac{q_i q_j^{\text{eff}}}{r_{ij}} f_{\text{Thole}}(r_{ij}) \\ & + \sum_{i\in \text{water}} \sum_{j \in \text{WI in TiO}_2} \frac{q_i q_j}{r_{ij}} f_{\text{Thole}}(r_{ij}) \\ & + \frac{1}{2} \sum_{i,j} V_i K_{ij} V_j \end{aligned} \tag{21}$$

Here, q^{eff} is an effective site charge at an atom site in the TiO_2, to which the polarization effect arising from the bulk TiO_2 is renormalized. q^{eff} is given by the nonpolarizable force field in ref 15. The second term in eq 21 represents the interaction between site charges of water and induced charges at the WI sites of the TiO_2. The WI site charges in the TiO_2 are zero without an external electric field and are induced only by an electric field of water. The charges for the TiO_2 surface are summarized in Table 2. Calculation of the CRK parameters for the TiO_2 surface will be presented in the next section. The intramolecular water potential $V_{\text{water–intra}}$ is given by ref 43.

III.B. Determination of CRK Parameters of TiO_2 Surface. We performed first-principles calculations of a slab TiO_2 system with the dipole-correction method. The SIESTA package program[44] was employed for the electronic structure calculations. The procedure of self-consistent dipole correction and calculation of induced charge were implemented on our in-house subprogram HiRUNE.[45−47] We used the Troullier−Martins norm-conserving pseudopotential[48] with the Kleinman−Bylander nonlocal projector.[49] We adopted the PBE functional[50] and the DZP level basis set. The k points were sampled by $4 \times 4 \times 1$. The minimum sample cell was set to the 1×2 unit cells of the rutile TiO_2 bulk, and the minimum sample slab consists of seven layers of the minimum sample cells. This cell size is necessary to model a water molecule adsorbed on the TiO_2 surface.[51] The lattice constants of a = 4.73 Å and c = 3.07 Å for the rutile TiO_2 crystal were used.[51] The (110) and (001) surfaces of the TiO_2 were optimized by fixing the atom positions of the five TiO_2 layers. Induced charge densities $\rho^{\text{ind}}(z)$ were computed by subtracting the charge density in the presence of an electric field from the charge density without an electric field.

The calculated $\rho^{\text{ind}}(z)$ and $E(z)$ are plotted in Figure 2. First, we shall discuss $\rho^{\text{ind}}(z)$ and $E(z)$ along the (110) direction. Figure 2a indicates that a positive charge is induced above the surface Ti layer ($z > 0$), while a relatively small negative charge is induced near the surface Ti layer. The Gaussian fits to $\rho^{\text{ind}}(z)$ are also shown in Figure 2a. To define the SCRK in the TiO_2 surface region, the two surfaces Z_b and Z_s were set at the peak positions of Gaussian fits. For the bulk TiO_2 region ($z < 0$), the minimum sample cell was assumed to be a uniform continuous medium. Hence, the charge density in the minimum sample cell was averaged, and two identical surfaces Z were set for each minimum sample cell. This is schematically shown in Figure 2c. The induced surface charges calculated from eq 9 were $q_{Zb}{}^{\text{ind}}$ = 0.2877e and $q_{Zs}{}^{\text{ind}}$ = 0.0580e, while we set $q_Z{}^{\text{ind}}$ = 0e. Figure 2b shows that E in the vacuum region was 0.0153 au. From eq 10, we obtained the off-diagonal SCRK of $K_{ZbZs}{}^{\text{SCRK}}$ = 7.602 au, $K_{ZsZ}{}^{\text{SCRK}}$ = 4.651 au, and $K_{ZZ'}{}^{\text{SCRK}}$ = 2.325 au. Similarly, we calculated the SCRK along the (001) direction. The induced surface charge was 0.1742e, and the external electric field was 0.0172 au, providing the off-diagonal SCRK of $K_{YY'}{}^{\text{SCRK}}$ = 1.743 au for the bulk TiO_2.

Next, the SCRK was mapped onto the CRK (see Figure 1). We defined three types of the WI sites, W_b, W_s, and W, corresponding to the surfaces Z_b, Z_s, and Z, respectively. The bulk WI (W) is defined by the center of mass for six titanium atoms (six Ti atoms or three Ti, two Ti_{VI}, one Ti_V) and six oxygen atoms (six O atoms or two O, O_s, O_u atoms) in a unit cell. W_s is located on the Ti surface layer and is defined by the center of mass for two Ti_{VI}, one Ti_V and two O_s atoms. W_b is located at the O_b atom position. These WIs are schematically shown in Figure 3. First, we map the SCRK of $K_{ZZ'}$ and $K_{YY'}$ to the CRK for the W sites in the bulk. Since $K_{ZZ'}{}^{\text{SCRK}}$ can be mapped onto the sum of four $K_{z,\text{WW}'}$, $K_{z,\text{WW}'} = K_{ZZ'}{}^{\text{SCRK}}/4$, where $K_{z,\text{WW}'}$ is the CRK between the W and W′ sites in the (110) direction. Since the (110) and (1$\bar{1}$0) directions are identical, $K_{z,\text{WW}'} = K_{x,\text{WW}'}$. Similarly, we have $K_{y,\text{WW}'} = K^{\text{SCRK}}{}_{YY'}/4$, where $K_{y,\text{WW}'}$ is the CRK in the (001) direction. We consider the CRK associated with the W_s and W_b sites. Since $K_{ZsZ}{}^{\text{SCRK}}$ can be mapped onto the sum of four $K_{z,\text{WsW}}$, we have $K_{z,\text{WsW}} = K_{ZsZ}{}^{\text{SCRK}}/4$. On the other hand, half of $K_{YY'}{}^{\text{SCRK}}$ can be mapped onto the sum of four $K_{y,\text{WsW}}$, thus, $K_{y,\text{WsW}} = K_{YY'}{}^{\text{SCRK}}/8$. Similarly, $K_{x,\text{WsW}}$ is equal to $K_{ZsZ}{}^{\text{SCRK}}/8$. The CRK associated with the W_b site is more complicated than that of W_s. Because the W_s−W_b is not parallel to either the surface or the surface normal, K_{WbWs} should be represented by the combination of SCRKs

dx.doi.org/10.1021/ct300998z | J. Chem. Theory Comput. 2013, 9, 1193−1201

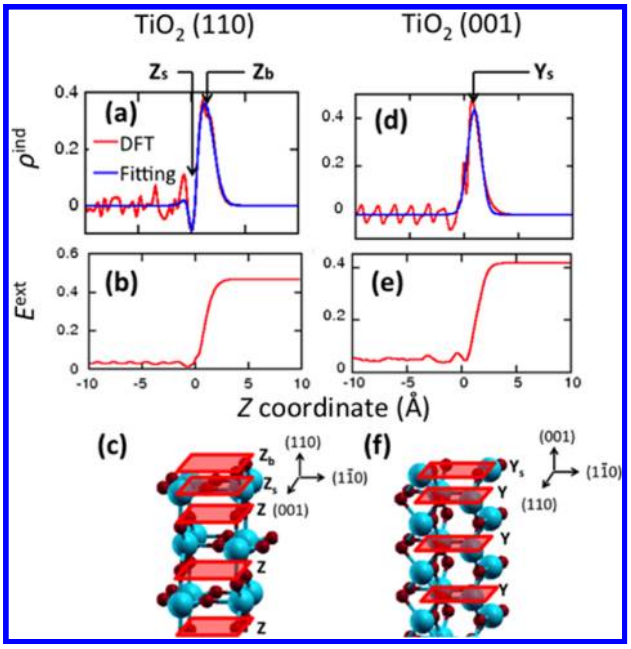

Figure 2. (a, d) Axial distributions of induced charge density obtained from the first-principles calculations. The Gaussian fits are also depicted. The origins of the z coordinates are defined as the surface Ti layer. The unit is the atomic unit. (b, e) Axial distributions of the electric fields in the atomic unit. (c, f) Schematic representations of the surfaces for the SCRK. Titanium and oxygen atoms are represented by sky blue and dark red spheres, respectively. The calculation results for the $TiO_2(110)$ and (001) slab models are shown in a, b, and c and in d, e, and f, respectively.

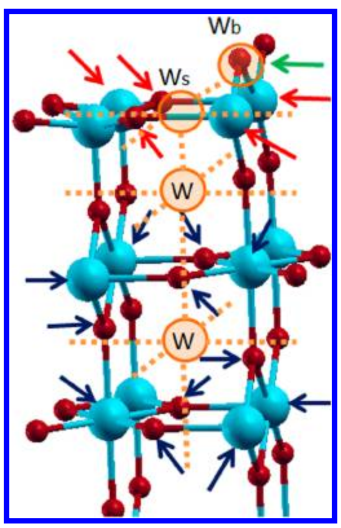

Figure 3. Schematic representation of the CRK sites. Titanium and oxygen atoms are represented by sky blue and dark red spheres, respectively, while the CRK sites are represented by orange circles. The W_b site is located at the position of the O_b atom indicated by a green arrow. The W_s site is the center of mass for three titanium and two oxygen atoms indicated by red arrows, and the W site is the center of mass for six titanium and six oxygen atoms indicated by blue arrows.

parallel and perpendicular to the surface. K_{WbWs} was, then, assumed to be given by

$$K_{\mathrm{WbWs}} = \sqrt{\left(\frac{\cos\theta K_{\mathrm{ZsZb}}^{\mathrm{SCRK}}}{4}\right)^2 + \left(\frac{\sin\theta K_{\mathrm{YY'}}^{\mathrm{SCRK}}}{8}\right)^2} \tag{22}$$

where the angle θ is formed by W_s−W_b and the z axis. The diagonal CRK parameters can be calculated by

$$K_{ii} = -\sum_{j\neq i} K_{ij} \tag{23}$$

We have presented a novel method to calculate the CRK representing the TiO_2 surface polarization where the CRK parameters are obtained from the first-principles calculations. However, the combination of the polarizable electrostatic interactions described by the CRK with the nonpolarizable Lennard-Jones potential often causes the divergence of induced charges in the MD simulations. To avoid this divergence, the repulsive Lennard-Jones potential parameters should be increased[32] or the CRK should be scaled down.[43] In the present study, the CRK parameters obtained by the first-principles calculations were scaled down by 27%.[43] The obtained off-diagonal CRK parameters are listed in Table 3.

Finally, we briefly note the limitation and extension of the present force-field model. We applied a uniform electric field to the clean surface TiO_2 slab and calculated the SCRK based on the first principles calculations. Therefore, the explicit charge transfer between water molecule and TiO_2 is not considered. Each water molecule is always neutral while the surface region of TiO_2 is not necessarily neutral by induced charge. When one focuses on the dissociative adsorption of water or surface with oxygen vacancies, the present model should be extended to represent charge transfer between adsorbed moieties and surface. Such extension is straightforward in our theoretical scheme. The minimum sample slab is set as the system including adsorbed moieties, e.g., containing OH terminal on TiO_2. Then, the same procedure is applicable to determining CRK, which represents charge transfer from/to adsorbates.

IV. COMPARISON WITH THE FIRST-PRINCIPLES CALCULATIONS FOR A SINGLE WATER MOLECULE ON THE TiO_2 SURFACE

To check the accuracy of our force-field model, we compared the optimized geometries and the induced charges for a system of water adsorbed on the TiO_2 (110) surface between the force-field model and first principles calculations. For the first-principles calculations, we prepared a system of one water molecule adsorbed on the 1 × 1 minimum sample slab of the TiO_2. The structure of the system was optimized by fixing the atom positions for the five TiO_2 layers. To prevent the plane of the water molecule from lying parallel to the TiO_2 surface, the water atoms were enforced to have the same y coordinate. We also prepared a corresponding system of nine water molecules attached to the 3 × 3 minimum sample slab of the TiO_2 for the force-field model calculations. The simulation cell sizes of the x and y axes were 20.07 Å and 18.44 Å, respectively, while the cell size along the z axis was set to 120 Å. The periodic boundary condition was used for the x and y directions, while the reflection wall was set for the z direction. The electrostatic interaction was calculated by using the isotropic periodic sum method with a cutoff of 45 Å.[52−54] Note that the periodicity of water structure was enforced in the 3 × 3 minimum sample cell so that a system used in the force field calculation is consistent with that for the first-principles calculation.

First, we calculated the nearest neighbor distance between the H_w and the O_b atoms, $r_{\mathrm{Hw-Ob}}$, and between the O_w and the Ti_V atoms, $r_{\mathrm{Ow-TiV}}$, for these optimized structures. By using our force-field model, we obtained $r_{\mathrm{Hw-Ob}}$ = 1.89 Å and $r_{\mathrm{Ow-TiV}}$ = 2.32 Å,

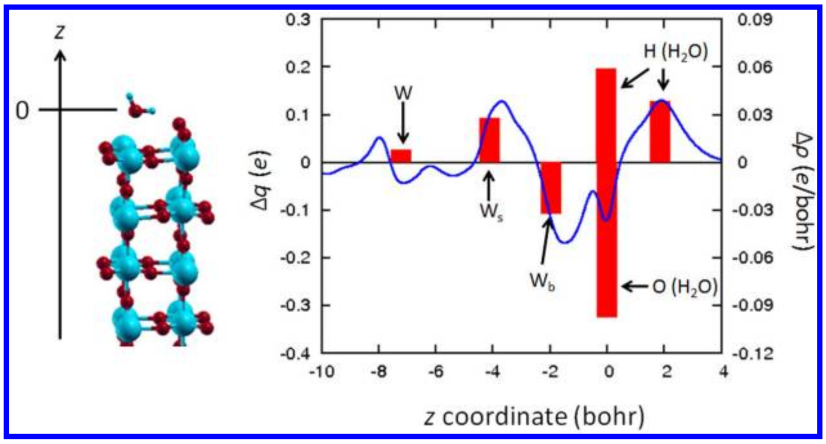

Figure 4. (Left) Optimized structure of a water molecule attached to the rutile $TiO_2(110)$ surface by using the first-principles calculations. (Right) Induced site charges calculated by the CRK (red box plot) are compared with induced charge density obtained from the first-principles calculations (blue curve). The origin of the z coordinate was set to the position of the O_w atom.

while our first-principles calculations provided $r_{Hw-Ob} = 1.79$ Å and $r_{Ow-TiV} = 2.33$ Å. This indicates that our polarizable force-field model can reproduce r_{Ow-TiV} well. Since the PBE functional consistently underestimated the hydrogen bond length,[55] we concluded that $r_{Hw-Ob} = 1.89$ Å predicted by our polarizable model was reasonable. Note that the nonpolarizable simulation provided $r_{Hw-Ob} = 1.73$ Å and $r_{Ow-TiV} = 2.17$ Å.[16]

The charges induced by the water−TiO_2 interactions were also compared with the first-principles calculation. The induced charge density was calculated

$$\Delta\rho(z) = \rho_{TiO_2-water}(z) - \rho_{TiO_2}(z) - \rho_{water}(z) \tag{24}$$

where $\rho_{TiO_2-water}$, ρ_{water}, and ρ_{TiO_2} denote the charge density of water attached to the TiO_2 surface, isolated water system without the TiO_2 surface, and the TiO_2 surface without water, respectively. The induced site charges corresponding to eq 24 can be calculated from our polarizable force-field model as

$$\Delta q_i = q_i - q_i^{(0)} \tag{25}$$

The comparison of the induced charges is shown in Figure 4. Our polarizable model indicates that a negative charge is induced at the W_b site because of the H_w atom attached to the O_b atom, and a positive charge is induced at the W_s site because of the O_w atom attached to the Ti_v atom, while a small charge is induced at the W site. These tendencies are in good agreement with the first-principles calculation. This indicates that our polarizable force field reproduces the geometry of water attached to the TiO_2 surface predicted by the first-principles calculation as well as the charges induced by the water−TiO_2 electrostatic interactions.

V. APPLICATION TO LIQUID WATER AND THE RUTILE $TiO_2(110)$ SURFACE

In the previous section, we considered a system consisting of water adsorbed on the TiO_2 surface in the gas phase. Here, we apply our force field to the *liquid* water/TiO_2 interface. A system consisted of 512 water molecules and the 3 × 3 minimum sample slab of the rutile $TiO_2(110)$ surface. The RESPA algorithm was used for integrating equations of motion,[56] where the forces associated with the intramolecular potential of water were calculated every 0.125 fs and the other forces were calculated every 1.0 fs. We set the system temperature at 300 K in the microcanonical ensemble. A 100 ps MD run was performed to equilibrate the system, and a sequential 300 ps MD run was performed for sampling the trajectory. The snapshot of the simulated water/TiO_2 interface is shown in Figure 5.

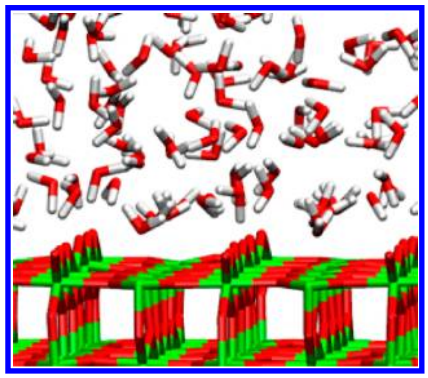

Figure 5. Snapshot of the water/clean rutile $TiO_2(110)$ interface.

We calculated the axial density distributions of the O_w and H_w atoms, which were summarized in Figure 6. A sharp peak of the O_W density distribution is located at $z = 2.2$ Å, which is in good agreement with the previous study with the nonpolarizable force field.[3] This peak corresponds to water with the O_w atom attached to the Ti_v atom. This is schematically illustrated in Figure 6. In contrast to the $z = 2.2$ Å peak, the peak at $z = 3.8$ Å reported in ref 3 is split into two peaks in Figure 6; a peak at $z = 3.4$ Å corresponds to water with the H_w and O_w atoms interacting with the O_b atoms of the TiO_2 surface and the H_w atom of the other water molecule, respectively, and a peak at $z = 3.8$ Å corresponds to water with the H_w atom hydrogen bonded to the O_b atom. Although the peak at $z = 3.4$ Å is missing in the nonpolarizable force-field MD simulation,[3] the water molecules with $H_w\cdots O_b$ and $O_w\cdots H_w$ intermolecular interactions have been reported in the first-principles MD simulation.[6] This indicates that the water molecules with $H_w\cdots O_b$ and $O_w\cdots H_w$ intermolecular interactions are stabilized by the induced charges of water and TiO_2. Our polarizable force-field model predicts this water structure reasonably.

To perform an in-depth analysis for the different interfacial water structures between the polarizable and nonpolarizable force-field models, we checked the axial distributions of the induced charges for the O_w and H_w atoms. These are shown in Figure 7. The induced charge of the O_w atom is uniform and $-0.22e$ at $z > 7$ Å, while it increases with an approach to the TiO_2

dx.doi.org/10.1021/ct300998z | J. Chem. Theory Comput. 2013, 9, 1193−1201

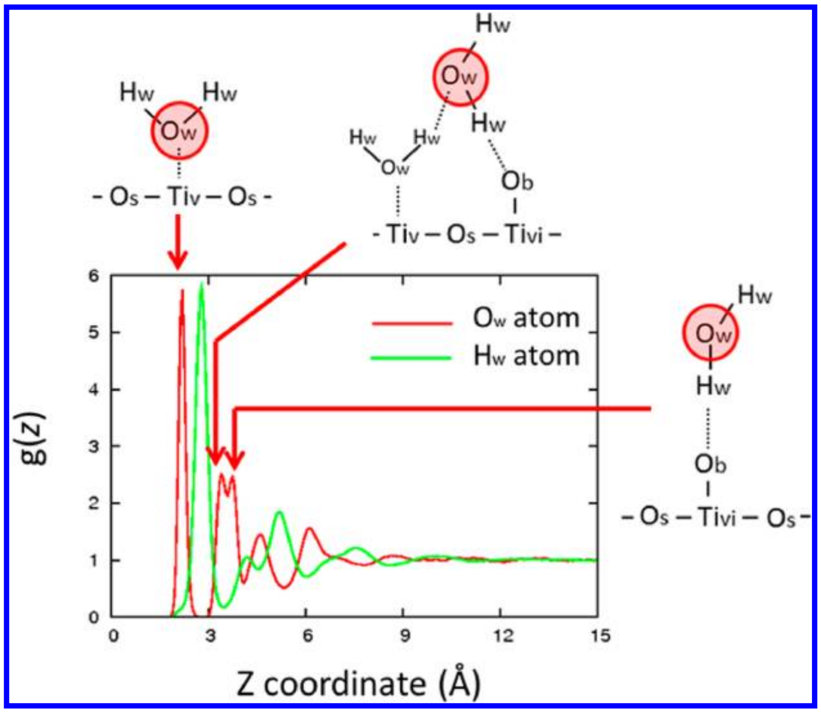

Figure 6. Axial density distributions $g(z)$ of the O_w and H_w atoms. The origin point is located at the surface Ti layer. The schematic pictures of water on the $TiO_2(110)$ surface contributing to the peaks of $g(z)$ are also illustrated.

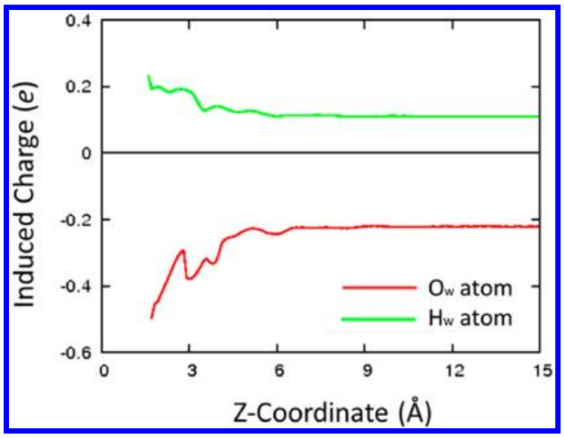

Figure 7. Induced charges for the O_w and H_w atoms. The origin point is located at the surface Ti layer.

surface. The water−TiO_2 interactions enhanced the induced charges of water, giving rise to stronger water−TiO_2 electrostatic interactions in the polarizable force-field model than in the nonpolarizable force-field model. The enhanced water−TiO_2 interactions stabilize the water molecules with the $H_w \cdots O_b$ and $O_w \cdots H_w$ intermolecular interactions.

VI. CONCLUDING REMARKS

We have presented a novel scheme to construct polarizable force fields applicable to the MD simulation at liquid/solid interfaces, which includes the surface polarity of solids by using the polarizable site charge model. This formalism allows us to implement a polarizable solid−liquid interaction potential into the conventional force fields easily. The CRK parameters in our model have been obtained from the first-principles calculations in a slab model with the help of the dipole-correction method. Our method was applied to the water/clean rutile $TiO_2(110)$ interface. The CRK sites in TiO_2 were located on the WI sites rather than the atom sites due to the delocalized electric nature of solids. The constructed force field model was tested by comparing the optimized structure and the depth distribution of the induced charge for a water molecule attached to the TiO_2 surface. We obtained good agreement between the force-field model and first-principles calculations.

We have simulated the *liquid* water/TiO_2 interface and have addressed the structures of water near the surface. Our MD simulation predicted three stable interfacial water structures; the O_w atom attached to the Ti_v atom, the H_w atom attached to the O_b atom, and the H_w and O_w atoms interacting with the O_b and H_w atoms, respectively. The former two structures have been predicted with the nonpolarizable model,[13,16] while the last structure has been predicted only by the first-principles MD simulations.[6] We analyzed the induced charges of water and found that the induced charges are dramatically enhanced at the interface due to the water−TiO_2 interactions, which stabilized the water molecules interacting with the O_b atom of the TiO_2 surface and the H_w atom of the other water. This indicates that the induced dipole dramatically enhanced at the water/TiO_2 interface has significant effects on the stable water structure near the TiO_2 surface.

The force field-based MD simulations are computationally less expensive than the first principles MD simulations and, thus, are suitable for monitoring the hydrogen bond dynamics and calculating the vibrational spectra such as sum frequency generation,[8,57,58] which requires over nanoseconds of MD simulations in a large system.[43,59] Studying water dynamics and the optical response of water near the TiO_2 surface is in progress.

■ AUTHOR INFORMATION

Corresponding Author

*E-mail: hs-nakamura@aist.go.jp, nagata@mpip-mainz.mpg.de.

Notes

The authors declare no competing financial interest.

■ ACKNOWLEDGMENTS

We appreciate Dr. R. K. Campen, Dr. A. C. Vila Verde, Dr. E. H. G. Backus, and Prof. M. Bonn for fruitful discussions. This research was supported by the Scientific Research on Innovative Areas, a MEXT Grant-in-Aid Project "Materials Design through Computics" (#23104514). T.O. thanks for the support from JSPS.

■ REFERENCES

(1) Fujishima, A.; Honda, K. Electrochemical photolysis of water at a semiconductor electrode. *Nature* **1972**, *238*, 37.

(2) Fujishima, A.; Zhang, X. T.; Tryk, D. A. TiO_2 photocatalysis and related surface phenomena. *Surf. Sci. Rep.* **2008**, *63*, 515.

(3) Cheng, H.; Selloni, A. Hydroxide ions at the water/anatase TiO_2(101) interface: Structure and electronic states from first principles molecular dynamics. *Langmuir* **2010**, *26*, 11518.

(4) Kowalski, P. M.; Meyer, B.; Marx, D. Composition, structure, and stability of the rutile TiO_2(110) surface: Oxygen depletion, hydroxylation, hydrogen migration, and water adsorption. *Phys. Rev. B* **2009**, *79*, 115410.

(5) Liu, L. M.; Zhang, C.; Thornton, G.; Michaelides, A. Reply to Comment on "Structure and dynamics of liquid water on rutile TiO_2(110)". *Phys. Rev. B* **2012**, *85*, 167402.

(6) Liu, L. M.; Zhang, C. J.; Thornton, G.; Michaelides, A. Structure and dynamics of liquid water on rutile TiO_2(110). *Phys. Rev. B* **2010**, *82*, 161415.

(7) Sumita, M.; Hu, C. P.; Tateyama, Y. Interface water on TiO_2 anatase (101) and (001) surfaces: First-principles study with TiO_2 slabs dipped in bulk water. *J. Phys. Chem. C* **2010**, *114*, 18529.

(8) Tilocca, A.; Selloni, A. Vertical and lateral order in adsorbed water layers on anatase TiO_2(101). *Langmuir* **2004**, *20*, 8379.

(9) Tilocca, A.; Selloni, A. Structure and reactivity of water layers on defect-free and defective anatase TiO_2(101) surfaces. *J. Phys. Chem. B* **2004**, *108*, 4743.

(10) Wesolowski, D. J.; Sofo, J. O.; Bandura, A. V.; Zhang, Z.; Mamontov, E.; Predota, M.; Kumar, N.; Kubicki, J. D.; Kent, P. R. C.; Vlcek, L.; Machesky, M. L.; Fenter, P. A.; Cummings, P. T.; Anovitz, L. M.; Skelton, A. A.; Rosenqvist, J. Comment on "Structure and dynamics of liquid water on rutile TiO_2(110)". *Phys. Rev. B* **2012**, *85*, 167401.

(11) Cheng, J.; Sprik, M. Aligning electronic energy levels at the TiO_2/H_2O interface. *Phys. Rev. B* **2010**, *82*, 081406.

(12) Cheng, J.; Sprik, M. Acidity of the aqueous rutile TiO_2(110) surface from density functional theory based molecular dynamics. *J. Chem. Theory Comput.* **2010**, *6*, 880.

(13) Predota, M.; Bandura, A. V.; Cummings, P. T.; Kubicki, J. D.; Wesolowski, D. J.; Chialvo, A. A.; Machesky, M. L. Electric double layer at the rutile (110) surface. 1. Structure of surfaces and interfacial water from molecular dynamics by use of ab initio potentials. *J. Phys. Chem. B* **2004**, *108*, 12049.

(14) Predota, M.; Cummings, P. T.; Wesolowski, D. J. Electric double layer at the rutile (110) surface. 3. Inhomogeneous viscosity and diffusivity measurement by computer simulations. *J. Phys. Chem. C* **2007**, *111*, 3071.

(15) Alimohammadi, M.; Fichthorn, K. A. A force field for the interaction of water with TiO_2 surfaces. *J. Phys. Chem. C* **2011**, *115*, 24206.

(16) Bandura, A. V.; Kubicki, J. D. Derivation of force field parameters for TiO_2-H_2O systems from a initio calculations. *J. Phys. Chem. B* **2003**, *107*, 11072.

(17) Johnston, K.; Herbers, C. R.; van der Vegt, N. F. A. Development of Classical Molecule−Surface Interaction Potentials Based on Density Functional Theory Calculations: Investigation of Force Field Representability. *J. Phys. Chem. C* **2012**, *116*, 19781.

(18) Head-Gordon, M.; Tully, J. C. Vibrational-relaxation on metal-surfaces - molecular-orbital theory and application to CO/Cu(100). *J. Chem. Phys.* **1992**, *96*, 3939.

(19) Wang, X. G.; Chaka, A.; Scheffler, M. Effect of the environment on alpha-Al_2O_3 (0001) surface structures. *Phys. Rev. Lett.* **2000**, *84*, 3650.

(20) Giovambattista, N.; Debenedetti, P. G.; Rossky, P. J. Effect of surface polarity on water contact angle and interfacial hydration structure. *J. Phys. Chem. B* **2007**, *111*, 9581.

(21) Hallil, A.; Tetot, R.; Berthier, F.; Braems, I.; Creuze, J. Use of a variable-charge interatomic potential for atomistic simulations of bulk, oxygen vacancies, and surfaces of rutile TiO_2. *Phys. Rev. B* **2006**, *73*, 165406.

(22) Han, X. J.; Bergqvist, L.; Dederichs, P. H.; Muller-Krumbhaar, H.; Christie, J. K.; Scandolo, S.; Tangney, P. Polarizable interatomic force field for TiO_2 parametrized using density functional theory. *Phys. Rev. B* **2010**, *81*, 134108.

(23) Ogata, S.; Iyetomi, H.; Tsuruta, K.; Shimojo, F.; Kalia, R. K.; Nakano, A.; Vashishta, P. Variable-charge interatomic potentials for molecular-dynamics simulations of TiO_2. *J. Appl. Phys.* **1999**, *86*, 3036.

(24) Swamy, V.; Gale, J. D.; Dubrovinsky, L. S. Atomistic simulation of the crystal structures and bulk moduli of TiO_2 polymorphs. *J. Phys. Chem. Solids* **2001**, *62*, 887.

(25) Swamy, V.; Muscat, J.; Gale, J. D.; Harrison, N. M. Simulation of low index rutile surfaces with a transferable variable-charge Ti-O interatomic potential and comparison with ab initio results. *Surf. Sci.* **2002**, *504*, 115.

(26) Cornell, W. D.; Cieplak, P.; Bayly, C. I.; Gould, I. R.; Merz, K. M.; Ferguson, D. M.; Spellmeyer, D. C.; Fox, T.; Caldwell, J. W.; Kollman, P. A. A 2nd generation force-field for the simulation of proteins, nucleic-acids, and organic-molecules. *J. Am. Chem. Soc.* **1995**, *117*, 5179.

(27) Jorgensen, W. L.; Maxwell, D. S.; TiradoRives, J. Development and testing of the OPLS all-atom force field on conformational energetics and properties of organic liquids. *J. Am. Chem. Soc.* **1996**, *118*, 11225.

(28) MacKerell, A. D.; Bashford, D.; Bellott, M.; Dunbrack, R. L.; Evanseck, J. D.; Field, M. J.; Fischer, S.; Gao, J.; Guo, H.; Ha, S.; Joseph-McCarthy, D.; Kuchnir, L.; Kuczera, K.; Lau, F. T. K.; Mattos, C.; Michnick, S.; Ngo, T.; Nguyen, D. T.; Prodhom, B.; Reiher, W. E.; Roux, B.; Schlenkrich, M.; Smith, J. C.; Stote, R.; Straub, J.; Watanabe, M.; Wiorkiewicz-Kuczera, J.; Yin, D.; Karplus, M. All-atom empirical potential for molecular modeling and dynamics studies of proteins. *J. Phys. Chem. B* **1998**, *102*, 3586.

(29) Morita, A.; Kato, S. Ab initio molecular orbital theory on intramolecular charge polarization: Effect of hydrogen abstraction on the charge sensitivity of aromatic and nonaromatic species. *J. Am. Chem. Soc.* **1997**, *119*, 4021.

(30) Morita, A.; Kato, S. Molecular dynamics simulation with the charge response kernel: Diffusion dynamics of pyrazine and pyrazinyl radical in methanol. *J. Chem. Phys.* **1998**, *108*, 6809.

(31) Isegawa, M.; Kato, S. Polarizable force field for protein with charge response kernel. *J. Chem. Theory Comput.* **2009**, *5*, 2809.

(32) Iuchi, S.; Morita, A.; Kato, S. Molecular dynamics simulation with the charge response kernel: Vibrational spectra of liquid water and N-methylacetamide in aqueous solution. *J. Phys. Chem. B* **2002**, *106*, 3466.

(33) Nagata, Y. Polarizable atomistic calculation of site energy disorder in amorphous Alq_3. *Chemphyschem* **2010**, *11*, 474.

(34) Nakano, H.; Yamamoto, T.; Kato, S. A wave-function based approach for polarizable charge model: Systematic comparison of polarization effects on protic, aprotic, and ionic liquids. *J. Chem. Phys.* **2010**, *132*, 044106.

(35) Bengtsson, L. Dipole correction for surface supercell calculations. *Phys. Rev. B* **1999**, *59*, 12301.

(36) Meyer, B.; Vanderbilt, D. Ab initio study of $BaTiO_3$ and $PbTiO_3$ surfaces in external electric fields. *Phys. Rev. B* **2001**, *63*, 205426.

(37) Vanderbilt, D.; Kingsmith, R. D. Electric polarization as a bulk quantity and its relation to surface-charge. *Phys. Rev. B* **1993**, *48*, 4442.

(38) Thole, B. T. Molecular polarizable calculated with a modified dipole interaction. *Chem. Phys.* **1981**, *59*, 341.

(39) Ghosez, P.; Michenaud, J. P.; Gonze, X. Dynamical atomic charges: The case of ABO_3 compounds. *Phys. Rev. B* **1998**, *58*, 6224.

(40) Giustino, F.; Pasquarello, A. Theory of atomic-scale dielectric permittivity at insulator interfaces. *Phys. Rev. B* **2005**, *71*, 144104.

(41) Stengel, M. Electrostatic stability of insulating surfaces: Theory and applications. *Phys. Rev. B* **2011**, *84*, 205432.

(42) Tasker, P. W. Stability of ionic-crystal surfaces. *J. Phys. C: Solid. State Phys.* **1979**, *12*, 4977.
(43) Nagata, Y.; Mukamel, S. Vibrational sum-frequency generation spectroscopy at the water/lipid interface: Molecular dynamics simulation study. *J. Am. Chem. Soc.* **2010**, *132*, 6434.
(44) Soler, J. M.; Artacho, E.; Gale, J. D.; Garcia, A.; Junquera, J.; Ordejon, P.; Sanchez-Portal, D. The SIESTA method for ab initio order-N materials simulation. *J. Phys.: Consens. Matter* **2002**, *14*, 2745.
(45) Nakamura, H.; Yamashita, K.; Rocha, A. R.; Sanvito, S. Efficient ab initio method for inelastic transport in nanoscale devices: Analysis of inelastic electron tunneling spectroscopy. *Phys. Rev. B* **2008**, *78*, 235420.
(46) Ohto, T.; Yamashita, K.; Nakamura, H. First-principles study of electronic structure and charge transport at PTCDA molecular layers on Ag(111) and Al(111) electrodes. *Phys. Rev. B* **2011**, *84*, 045417.
(47) Nakamura, H.; Asai, Y.; Hihath, J.; Bruot, C.; Tao, N. Switch of conducting orbital by bias-induced electronic contact asymmetry in a bipyrimidinyl-biphenyl diblock molecule: Mechanism to achieve a pn directional molecular diode. *J. Phys. Chem. C* **2011**, *115*, 19931.
(48) Troullier, N.; Martins, J. L. Efficient pseudopotentials for plane-wave calculations. *Phys. Rev. B* **1991**, *43*, 1993.
(49) Kleinman, L.; Bylander, D. M. Efficacious form for model pseudopotentials. *Phys. Rev. Lett.* **1982**, *48*, 1425.
(50) Perdew, J. P.; Burke, K.; Ernzerhof, M. Generalized gradient approximation made simple. *Phys. Rev. Lett.* **1996**, *77*, 3865.
(51) Koitaya, T.; Nakamura, H.; Yamashita, K. First-Principle Calculations of Solvated Electrons at Protic Solvent-TiO_2 Interfaces with Oxygen Vacancies. *J. Phys. Chem. C* **2009**, *113*, 7236.
(52) Takahashi, K. Z.; Narumi, T.; Yasuoka, K. Cutoff radius effect of the isotropic periodic sum and Wolf method in liquid-vapor interfaces of water. *J. Chem. Phys.* **2011**, *134*, 174112.
(53) Wu, X. W.; Brooks, B. R. Isotropic periodic sum: A method for the calculation of long-range interactions. *J. Chem. Phys.* **2005**, *122*, 044107.
(54) Fukuda, I.; Nakamura, H. Non-Ewald methods: theory and applications to molecular systems. *Biophys. Rev.* **2012**, *4*, 161.
(55) Ireta, J.; Neugebauer, J.; Scheffler, M. On the accuracy of DFT for describing hydrogen bonds: Dependence on the bond directionality. *J. Phys. Chem. A* **2004**, *108*, 5692.
(56) Tuckerman, M.; Berne, B. J.; Martyna, G. J. Reversible multiple time scale molecular-dynamics. *J. Chem. Phys.* **1992**, *97*, 1990.
(57) Flores, S. C.; Kherb, J.; Konelick, N.; Chen, X.; Cremer, P. S. The effects of Hofmeister cations at negatively charged hydrophilic surfaces. *J. Phys. Chem. C* **2012**, *116*, 5730.
(58) Uosaki, K.; Yano, T.; Nihonyanagi, S. Interfacial water structure at as-prepared and UV-induced hydrophilic TiO_2 surfaces studied by sum frequency generation spectroscopy and quartz crystal microbalance. *J. Phys. Chem. B* **2004**, *108*, 19086.
(59) Ishiyama, T.; Morita, A. Vibrational spectroscopic response of intermolecular orientational correlation at the water surface. *J. Phys. Chem. C* **2009**, *113*, 16299.